Sensor and Simulation Notes

Note 400

August 1996

Design Optimization of Feed-Point Lenses for Half Reflector IRAs

W. Scott Bigelow
Everett G. Farr
Farr Research, Inc.

Gary D. Sower
EG&G, MSI

Abstract

A critical component of a high-voltage Half Impulse Radiating Antenna (HIRA) is the feed point lens, which is used to match an electrically large coaxial waveguide to the feed arms of the HIRA. The coaxial input interface is a prolate spheroidal (ellipse of revolution) surface; the output interface is a quartic surface. We derive equations for the design of this lens, subject to impedance matching constraints. We also derive a figure-of-merit for the lens design based on an aperture integral of the electric field. We provide solutions for two configurations based on these derivations. The most important result of these analyses is that the optimum design is an *oil-lens-air* configuration with a lens relative dielectric constant of 7.0.

I. Introduction

In [1] we developed design equations for the feed point lens used to match an electrically large coaxial waveguide to the feed arms of a high-voltage Half Impulse Radiating Antenna (HIRA). This lens, built from a single homogeneous dielectric material, converts a plane wave in the coaxial waveguide to a spherical wave launched onto the conical feed arms of the antenna. Although one would normally want to split the center conductor of the coaxial waveguide into two feed arms, we can only solve the problem semi-analytically for a rotationally symmetric geometry. For this reason, we assumed a single conical feed and an *F/D* ratio of 0.25, in order to maintain rotational symmetry. The solution to this case provides a good approximation to the less tractable three-dimensional problem.

Sketches of two possible lens designs, originally presented in [1], are shown in Figure I–1. We refer to the first design, which includes an oil cap, as an *oil-lens-oil* design. The second design, with no oil cap, simply has air or SF_6 at its output. This is an *oil-lens-air* design. The lens converts a plane wave in a coaxial geometry to a spherical wave in a conical geometry. The focus of the spherical wave is on the ground plane, at the center of the coaxial feed, and at the focus of a parabolic reflector.

In [1] we provided design equations that included both *oil-lens-oil* and *oil-lens-air* configurations. Examples based on those equations assumed input coaxial waveguide dimensions determined by high-voltage breakdown considerations. The impedance in oil was about 67 Ω, equivalent to 100 Ω in air. The matching lens output impedance was not enforced, and flare angle of the center conductor was unspecified. There remained three independent design parameters: (1) the dielectric constant of the lens, (2) the flare angle of the outer coaxial conductor in the transition to the output ground plane, and (3) the size of the hole in the output ground plane—the thickness of the lens scales with the size of this hole.

In this paper we extend the derivation of the lens equations presented in [1] to include enforcement of an output impedance matched to the input. This leads to a relationship between the first two design parameters cited above and to specification of the center conductor flare angle where it transitions to the conical output feed—both center and outer conductor shapes are determined. No new constraints are introduced concerning the size of the hole in the ground plane. The relationship between lens dielectric constant and outer conductor flare angle supplants the minimum flare angle introduced in [1] as arbiter of the minimum dielectric constant required for a viable lens design. We also provide here for design optimization based on maximizing the aperture integral of the electric field for the fast impulse. This leads to a choice of lens dielectric constant and corresponding outer conductor flare angle. We begin with incorporation of the output impedance condition into the lens design equations.

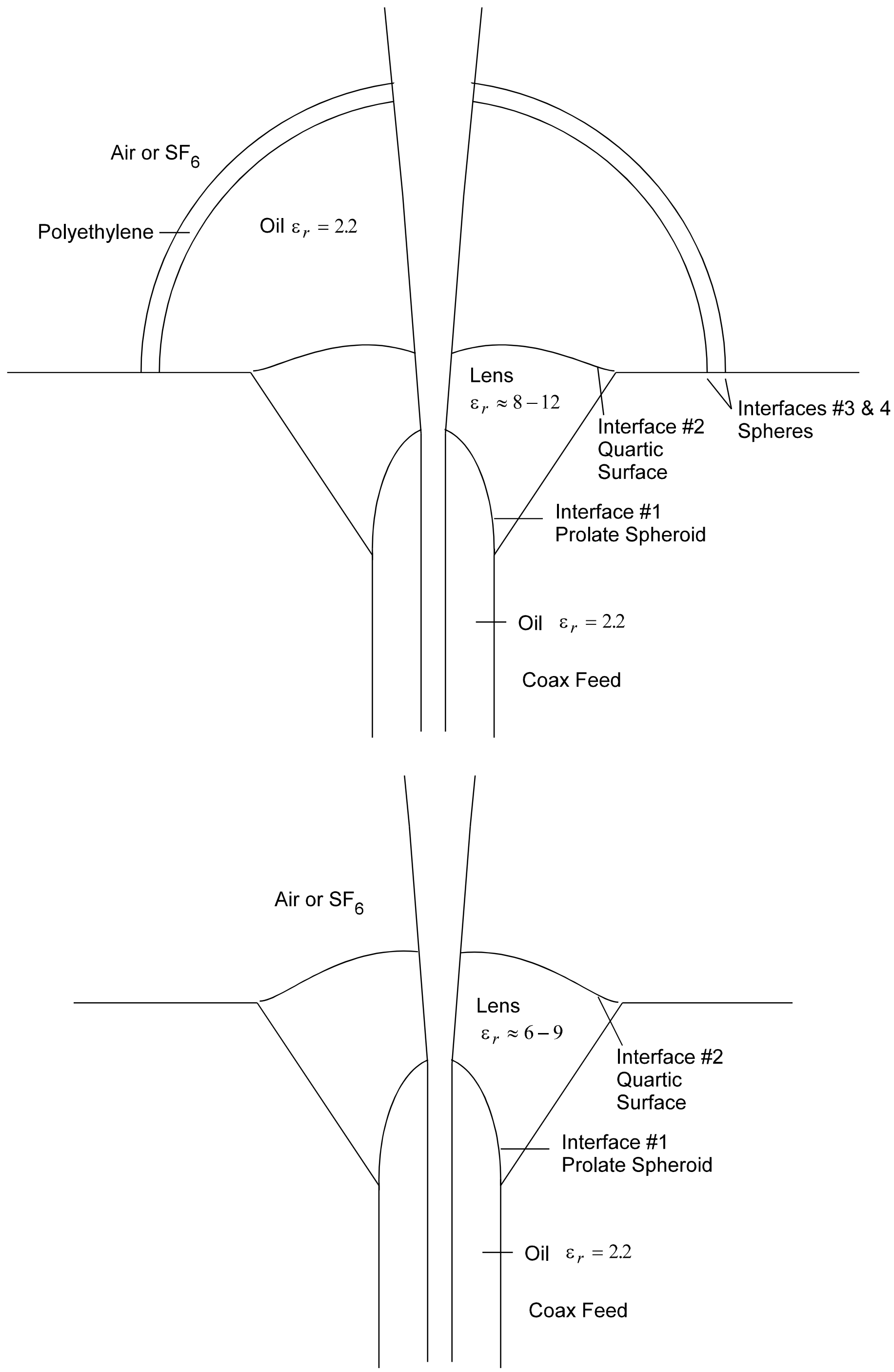

Figure I–1. An *oil-lens-oil* design (top), and an *oil-lens-air* design (bottom).

II. Imposition of the Output Impedance Condition

In the material that follows, we conform closely with the notation of [1]. We derive below a general expression for ℓ_2 / ℓ_1, and we use that expression along with previously derived results to incorporate a constraint in the lens design based on matching the output impedance of the lens to the impedance of the coaxial input waveguide. In following this material, it may be helpful to refer to the following figure, which amplifies the content of [1, Figure 3.1].

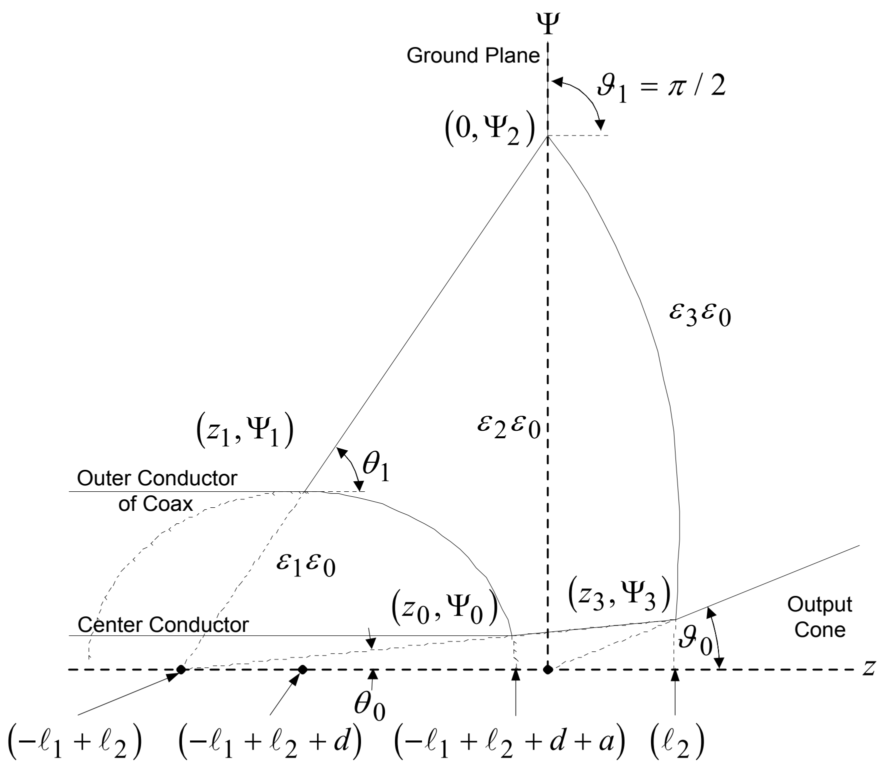

Figure II–1. Lens Design Parameters

In [1], we presented an equation for ℓ_2 / ℓ_1, based on the quartic equation for the lens-air interface, which involves the angle, θ_1, through which the extreme ray is bent by the ellipsoidal lens surface, and ε_{r2}, the ratio of the dielectric constant of the lens to the dielectric constant of the output medium—note that in [1], θ_1 was called $\Delta\theta_1$. A general expression for ℓ_2 / ℓ_1, valid for any ray initially traveling parallel to the axis of the coaxial input line can also be derived from the quartic equation ([1, (3.3)], reproduced below). That expression involves the angles through which such a ray is bent by both ellipsoidal and quartic lens surfaces. It also provides a means to relate the output impedance to other lens design parameters.

We begin our derivation with [1, (3.3)], the quartic equation

$$\sqrt{\varepsilon_{r2}}\left(-\ell_1+\sqrt{\Psi^2+(\ell_1-\ell_2+z)^2}\right)=-\ell_2+\sqrt{\Psi^2+z^2} \tag{2.1}$$

First, we divide through by Ψ to obtain

$$\sqrt{\varepsilon_{r2}}\left(-\frac{\ell_1}{\Psi}+\sqrt{1+\frac{(\ell_1-\ell_2+z)^2}{\Psi^2}}\right)=-\frac{\ell_2}{\Psi}+\sqrt{1+\frac{z^2}{\Psi^2}} \tag{2.2}$$

We next remove the explicit (z,Ψ) dependence by introducing two angles, θ and ϑ. The former, θ, is the angle by which a ray traveling axially in the coax region is bent as it passes through the ellipsoidal surface of the lens. It is a generalization of the angle, $\Delta\theta_1$, used in [1] and herein referred to simply as θ_1. The angle, ϑ, is the total bend angle experienced by the same ray after it has emerged from the quartic surface of the lens, which bends it by $\vartheta-\theta$. This ray, during its traverse of the lens at angle, θ, appears to originate at the left focus of the ellipsoid; upon emergence from the quartic, it appears to have originated at the coordinate system origin. From the geometry, we know that

$$\cot\theta=\frac{z+\ell_1-\ell_2}{\Psi} \quad \text{and} \quad \cot\vartheta=\frac{z}{\Psi} \tag{2.3}$$

We use these to eliminate the explicit z dependence from the quartic, obtaining

$$\sqrt{\varepsilon_{r2}}\left(-\frac{\ell_1}{\Psi}+\sqrt{1+\cot^2\theta}\right)=-\frac{\ell_2}{\Psi}+\sqrt{1+\cot^2\vartheta} \tag{2.4}$$

Next, the θ and ϑ equations (2.3) can be solved simultaneously to obtain Ψ as a function of θ and ϑ:

$$\Psi=\frac{-\ell_1+\ell_2}{\cot\vartheta-\cot\theta} \tag{2.5}$$

We now use this result to eliminate the remaining explicit Ψ dependence from the quartic. After making this substitution and using the trigonometric identity, $\csc^2\theta=1+\cot^2\theta$, we obtain:

$$\frac{\sqrt{\varepsilon_{r2}}}{1-\ell_2/\ell_1}(\cot\vartheta-\cot\theta)+\sqrt{\varepsilon_{r2}}\csc\theta=\frac{\ell_2/\ell_1}{1-\ell_2/\ell_1}(\cot\vartheta-\cot\theta)+\csc\vartheta \tag{2.6}$$

Since we have neither solved a quadratic nor introduced new quadratic terms in reaching this point, we choose the signs on the cosecant terms to match their sources in the original quartic. Now, we multiply through by $1-\ell_2/\ell_1$ and solve the resulting linear expression for the ratio ℓ_2/ℓ_1, finally obtaining

$$\frac{\ell_2}{\ell_1}=\frac{-\csc\vartheta+\sqrt{\varepsilon_{r2}}\,(\cot\vartheta-\cot\theta+\csc\theta)}{-\csc\vartheta+\cot\vartheta-\cot\theta+\sqrt{\varepsilon_{r2}}\,\csc\theta} \tag{2.7}$$

The general expression for ℓ_2/ℓ_1 obtained above can be used to relate the lens design parameters to the desired output impedance of the lens. The output impedance can be related to the angles ϑ and θ for the paraxial ray ($\Psi=\Psi_0$ in the coaxial region) and for the extreme ray ($\Psi=\Psi_1$), respectively. The paraxial ray is bent through an angle of $\theta=\theta_0$ at the first interface and emerges from the second interface at an angle of $\vartheta=\vartheta_0$ with respect to the axis. The extreme ray is bent through an angle of $\theta=\theta_1$ at the first interface and emerges from the second interface at an angle of $\vartheta=\pi/2$, parallel to the ground plane at $z=0$. The output impedance is that of a monocone, with cone angle ϑ_0, over a ground plane. We need to solve for the lens parameters consistent with these constraints for the desired impedance of Z_{coax}^{air}. This impedance is determined by the output cone angle, ϑ_0. Thus, we solve the following impedance expression for the cone angle

$$Z_3\sqrt{\varepsilon_3}=Z_{coax}^{air}=\frac{Z_0}{2\pi}\ln\left(\cot\frac{\vartheta_0}{2}\right) \tag{2.8}$$

where Z_0, is the impedance of free space, $376.727\,\Omega$.

This result can now be used with the general expression for ℓ_2/ℓ_1, evaluated at $\theta=\theta_0$ and $\vartheta=\vartheta_0$, to obtain an expression in which the unknowns are ℓ_2/ℓ_1 and θ_0

$$\frac{\ell_2}{\ell_1}=\frac{-\csc\vartheta_0+\sqrt{\varepsilon_{r2}}\,(\cot\vartheta_0-\cot\theta_0+\csc\theta_0)}{-\csc\vartheta_0+\cot\vartheta_0-\cot\theta_0+\sqrt{\varepsilon_{r2}}\,\csc\theta_0} \tag{2.9}$$

Although we could use [1, (3.3)] to provide an equation relating θ_1 and ℓ_2/ℓ_1, we can obtain an equivalent relationship by evaluating (2.7) at $\theta=\theta_1$ and $\vartheta=\pi/2$

$$\frac{\ell_2}{\ell_1}=\frac{-1+\sqrt{\varepsilon_{r2}}\,(-\cot\theta_1+\csc\theta_1)}{-1-\cot\theta_1+\sqrt{\varepsilon_{r2}}\,\csc\theta_1} \tag{2.10}$$

By equating these two expressions for ℓ_2 / ℓ_1, we can eliminate ℓ_2 / ℓ_1, leaving a single equation for the two unknown angles, θ_0 and θ_1. An independent equation relating θ_0 and θ_1 can be obtained by considering the impedance condition in the coaxial transmission line and a generalization of [1, (3.8)]. That generalization is

$$\frac{a}{\Psi} = \frac{\sqrt{\varepsilon_{r1}}}{\varepsilon_{r1} - 1}\left(\cot\theta + \sqrt{\varepsilon_{r1}}\csc\theta\right) \tag{2.11}$$

where a is the semi-major axis of the ellipsoidal lens surface, ε_{r1} is the ratio of the dielectric constant of the lens to the dielectric constant of the input medium (oil), and θ is the bend angle of a ray traveling parallel to the *z*-axis, which strikes the ellipsoidal lens surface at the radial coordinate, Ψ. Equation 3.8 of [1] is simply this expression evaluated at (θ_1, Ψ_1). Now, we also evaluate a / Ψ for the paraxial ray at (θ_0, Ψ_0), and form the ratio, $\left(a / \Psi_0\right) / \left(a / \Psi_1\right) = \Psi_1 / \Psi_0$, to obtain another equation relating θ_0 and θ_1

$$\frac{\Psi_1}{\Psi_0} = \frac{-\cot\theta_0 + \sqrt{\varepsilon_{r1}}\csc\theta_0}{-\cot\theta_1 + \sqrt{\varepsilon_{r1}}\csc\theta_1} = e^{2\pi f_g \sqrt{\varepsilon_1}} = e^{2\pi Z_{coax}^{air} / Z_0} \tag{2.12}$$

where we have also incorporated the coaxial line impedance result of [1, (5.3)]. Since the ratio, Ψ_1 / Ψ_0, is just a constant determined by the input impedance, we now have sufficient information to solve for θ_0, θ_1, and ℓ_2 / ℓ_1.

Summarizing, the equations to be solved for θ_0 and θ_1 are

$$\frac{-\csc\vartheta_0 + \sqrt{\varepsilon_{r2}}\left(\cot\vartheta_0 - \cot\theta_0 + \csc\theta_0\right)}{-\csc\vartheta_0 + \cot\vartheta_0 - \cot\theta_0 + \sqrt{\varepsilon_{r2}}\csc\theta_0} = \frac{-1 + \sqrt{\varepsilon_{r2}}\left(-\cot\theta_1 + \csc\theta_1\right)}{-1 - \cot\theta_1 + \sqrt{\varepsilon_{r2}}\csc\theta_1} \tag{2.13}$$

derived by equating the ℓ_2 / ℓ_1 expressions for paraxial and extreme rays, ((2.9), and (2.10)), and

$$\frac{-\cot\theta_0 + \sqrt{\varepsilon_{r1}}\csc\theta_0}{-\cot\theta_1 + \sqrt{\varepsilon_{r1}}\csc\theta_1} = e^{2\pi Z_{coax}^{air} / Z_0} \tag{2.14}$$

where

$$
\begin{aligned}
\varepsilon_1 &= 2.2 \quad \text{(dielectric constant of oil)} \\
\varepsilon_3 &= 1.0 \quad (\text{for an } \textit{oil - lens - air} \text{ design}) \\
&= 2.2 \quad (\text{ for an } \textit{oil - lens - oil} \text{ design}) \\
\varepsilon_{\text{r}1} &= \varepsilon_2 \,/\, \varepsilon_1 \text{ and } \varepsilon_{r2} = \varepsilon_2 \,/\, \varepsilon_3 \\
Z_{coax}^{air} &= Z_{output}^{air} = 100\,\Omega \text{ and } Z_0 = 376.737\Omega \\
\vartheta_0 &= 2\arctan\left(\exp\left(2\pi Z_{output}^{air} / Z_0\right)\right) \\
&= 2\arctan\left(\exp\left(200\pi/Z_0\right)\right) = 21.37 \text{ degrees}
\end{aligned}
\tag{2.15}
$$

For an assumed value of the lens dielectric constant, ε_2, equations(2.13) and (2.14) can be solved numerically for θ_0 and θ_1. In order to reduce the numerical solution process to a search for just one angle, θ_1, rather than both simultaneously, we eliminate θ_0 between these equations. To do so, we first make use of the substitutions

$$
\cot\theta = x \quad \text{and} \quad \csc\theta = \sqrt{1+x^2} \tag{2.16}
$$

These transform (2.12) and (2.13) into

$$
\begin{gathered}
\frac{-\csc\vartheta_0 + \sqrt{\varepsilon_{r2}}\left(\cot\vartheta_0 - x_0 + \sqrt{1+x_0^2}\right)}{-\csc\vartheta_0 + \cot\vartheta_0 - x_0 + \sqrt{\varepsilon_{r2}}\sqrt{1+x_0^2}} = \frac{-1+\sqrt{\varepsilon_{r2}}\left(-x_1 + \sqrt{1+x_1^2}\right)}{-1-x_1+\sqrt{\varepsilon_{r2}}\sqrt{1+x_1^2}} \\
\text{and} \quad \frac{-x_0 + \sqrt{\varepsilon_{r1}}\sqrt{1+x_o^2}}{-x_1+\sqrt{\varepsilon_{r1}}\sqrt{1+x_1^2}} = \mathrm{K}_Z
\end{gathered}
\tag{2.17}
$$

where $\mathrm{K}_Z = \exp\left(200\pi/Z_0\right)$. Next we solve the second of this pair of equations for x_0 and select the positive root, since a negative θ_0 is non-physical. The root is

$$
x_0 = \frac{-\mathrm{K}_Z\left(\left(\left(2x_1 - 2\sqrt{\varepsilon_{r1}}\sqrt{1+x_1^2}\right)\right) - \left(2x_1 - 2\sqrt{\varepsilon_{r1}}\sqrt{1+x_1^2}\right)\right)}{2\left(-1+\varepsilon_{r1}\right)}
\tag{2.18}
$$

$$
-2\left(\varepsilon_{r1} - \mathrm{K}_Z^2\left(\varepsilon_{r1} - x_1^2(1+\varepsilon_{r1}) + 2x_1\sqrt{\varepsilon_{r1}}\sqrt{1+x_1^2}\right)\right)
$$

We use this result to eliminate x_0 from the first equation of the (2.17) pair. The resulting expression can be solved numerically for x_1 by Newton's method. Then, x_0 can be obtained from (2.18); and θ_0 and θ_1 can be recovered as $\operatorname{arccot} x_0$ and $\operatorname{arccot} x_1$, respectively.

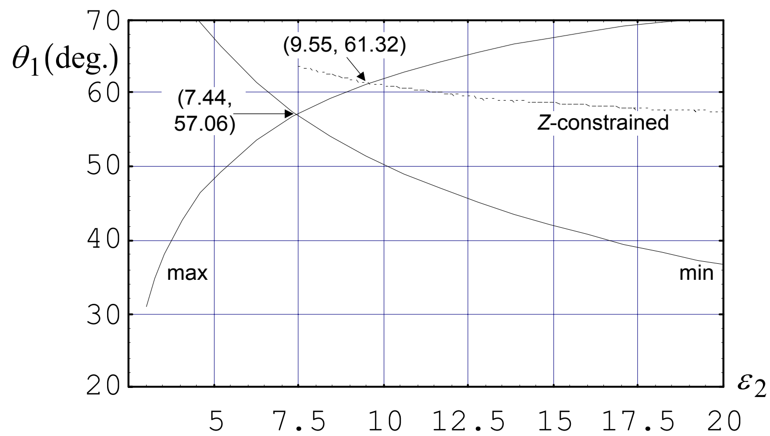

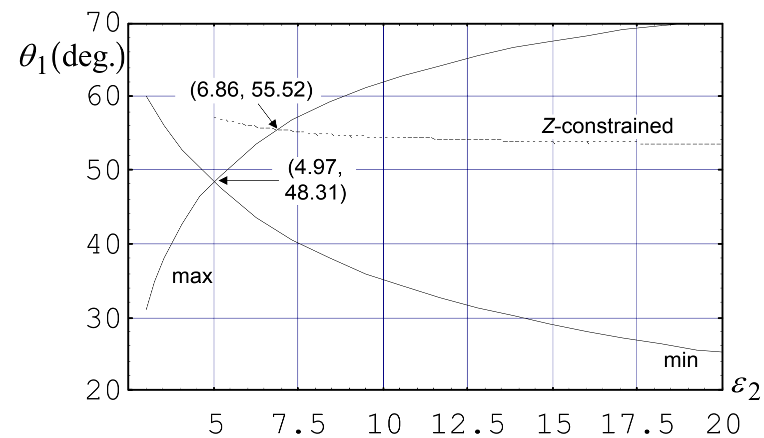

Figure II–2. Constraints on θ_1 and ε_2 for *oil-lens-oil* (top) and *oil-lens-air* (bottom) designs. Oil is assumed to have a dielectric constant of 2.2.

The angles θ_0 and θ_1 are determined by the choice of ε_2 and by the input (coaxial transmission line) impedance and output (cone over ground plane) impedance. The bend angle for the extreme ray, θ_1, is now a function of ε_2, as determined by the impedance constraints. This function is restricted to those values of θ_1 which lie between the maxima and minima given by [1, (4.2) and (4.6)]. From the accompanying graphs of these functions, we see that the minimum bend angle proves irrelevant. Whereas [1, (4.6)] assumed $\ell_2 / \ell_1 \to 0$, here, this ratio is determined by the impedance constraint. The maximum bend angle, in combination with the impedance constraint determines the minimum allowable ε_2.

At this point, the lens design is complete, save specification of the radius of the lens output, Ψ_2. The parameters of the ellipsoidal surface, *a*, *b*, and *d*, are obtained from (2.11) and from [1, (3.2)]. The ratio ℓ_2 / ℓ_1 is obtained from (2.7). The ratio, Ψ_2 / ℓ_1, is calculated by inversion of [1, (3.11)] as

$$\Psi_2 / \ell_1 = \frac{1 - \ell_2 / \ell_1}{\cot \theta_1} \tag{2.19}$$

A minimum for Ψ_2 is calculated from [1, (3.16)]. Selection of a suitable value, based on that constraint, completes the lens design specification for the assumed ε_2.

III. Lens Figure-of-Merit

An appropriate measure of performance of the lens is the aperture integral of the electric field for the fast impulse. A meaningful figure-of-merit for lens design must relate this aperture integral to the transmission coefficient for rays transmitted by the lens. Since the lens is symmetric about the *z*-axis, the transmission coefficient must possess the same rotational symmetry. Thus, all rays originating on a shell of constant radius, Ψ, in the coaxial waveguide feed will penetrate the lens and ultimately emerge in air with the same total transmission coefficient, $T_t(\Psi)$, the product of the Fresnel transmission coefficients for the ellipsoidal and quartic lens interfaces and for the spherical output (to air) interface, if applicable (see Figure I–1).

In Appendix A, we present a derivation which reduces the figure-of-merit calculation to evaluation of a single line integral of the transmission coefficient $T(u)$ along the y-axis in the aperture plane. There we use conformal mapping to show that the aperture plane integration can be replaced by integration over the radial coordinate, Ψ, in the coaxial input line. With minor changes in notation, the resulting figure-of-merit expression is

$$\boxed{\eta = \frac{h_{a,oil}}{h_{a,oil}^{(opt)}} = \frac{2/\Psi_1}{\sqrt[4]{\varepsilon_{oil}}} \int_{\Psi_0}^{\Psi_1} \frac{T_t(\Psi)}{(1+\Psi/\Psi_1)^2} d\Psi} \tag{3.1}$$

where $h_{a,oil}$ is the aperture integral of the electric field in the presence of transmission losses and $h_{a,oil}^{(opt)}$ is the optimal aperture integral, both normalized to the power in the oil-filled coax, as described in the appendix; ε_{oil} is the relative dielectric constant of oil. The figure-of-merit is a dimensionless quantity, expected to vary between zero and one. Lens design optimization consists of choosing parameters that maximize this figure-of-merit.

Given the lens properties and geometry, it is a straightforward process to calculate the required transmission coefficients from the Fresnel equations. The Fresnel transmission coefficients in terms of ray incidence angles at each lens interface can be converted to expressions dependent on Ψ in the coaxial line by application of Snell's law of refraction and by using the normal derivatives at the lens surfaces. This permits the above equation to be evaluated numerically to obtain the figure-of-merit for any choice of ε_2. We now describe this approach to obtaining $T_t(\Psi)$.

For E-plane incidence (electric field parallel to the plane of incidence), the Fresnel transmission coefficient at each interface is [2, p. 191]

$$T(\alpha_i) \;=\; \frac{2\,\sqrt{\varepsilon_i/\varepsilon_t}\,\cos(\alpha_i)}{\cos(\alpha_i)\,+\,\sqrt{\varepsilon_i/\varepsilon_t}\,\sqrt{1-(\varepsilon_i/\varepsilon_t)\sin^2(\alpha_i)}} \tag{3.2}$$

where α_i is the angle of incidence, ε_i is the dielectric constant in the medium of incidence, and ε_t is the dielectric constant in the medium of transmission. At the ellipsoidal lens interface, ε_i is ε_1 and ε_t is ε_2. At the quartic interface, ε_i is ε_2 and ε_t is ε_3. Since the output interface is assumed to be spherical and concentric with the wavefront, all rays are incident normally there; and the interface transmission coefficient reduces to

$$T_o \;=\; \frac{2}{1+\sqrt{\varepsilon_t/\varepsilon_i}} \tag{3.3}$$

Here, $\varepsilon_t = \varepsilon_{air}$ is always 1.0; and ε_i is ε_{oil} for an *oil-lens-oil* design and ε_{air} for an *oil-lens-air* design. Thus, $T_{o,oil-lens-oil} = 1.195$—the output transition is from oil to air—and $T_{o,oil-lens-air} = 1.0$—there is no output transition. The total transmission coefficient for a ray is just the product of the transmission coefficients at each of these interfaces.

Since the field in the coaxial input line is a plane wave, the rays there are traveling parallel to the *z*-axis; so the angle of incidence of each ray on the ellipsoidal lens surface is the same as the angle, $\alpha_{e,n}$, formed between the axis and the normal to the ellipse at that point, (z_e, Ψ_e). If such a ray is transmitted by the ellipsoidal surface, forming an angle, θ, with the *z*-axis, it will be incident upon the quartic surface at an angle, $\alpha_{q,i} = \theta - \alpha_{q,n}$, where $\alpha_{q,n}$ is the angle of the normal to the quartic surface at the point of incidence, (z_q, Ψ_q). Now, the angle of the normal to a curve at some point is just the angle whose cotangent is the negative of the slope at that point. Thus, the angles of incidence at ellipsoidal and quartic surfaces are given by

$$\begin{aligned}
\alpha_{e,i} &= \alpha_{e,n} = \operatorname{arccot}\left(-\left.\frac{\partial\Psi}{\partial z}\right|_e\right) \\
\alpha_{q,i} &= \theta - \alpha_{q,n} = \operatorname{arccot}\left(\frac{z_e - (-\ell_1 + \ell_2)}{\Psi_e}\right) - \operatorname{arccot}\left(-\left.\frac{\partial\Psi}{\partial z}\right|_q\right)
\end{aligned} \tag{3.4}$$

where the tangents to the ellipse and quartic are

$$\left.\frac{\partial \Psi}{\partial z}\right|_e = \frac{(b/a)^2}{\Psi}\left(-z+\left(-\ell_1+\ell_2+d\right)\right) \qquad \text{and}$$

$$\left.\frac{\partial \Psi}{\partial z}\right|_q = \frac{1}{\Psi}\left(-z+\frac{-\ell_1+\ell_2}{1+\dfrac{\sqrt{\left(z-\left(-\ell_1+\ell_2\right)\right)^2+\Psi^2}}{\sqrt{\varepsilon_{r2}}\sqrt{z^2+\Psi^2}}}\right) \tag{3.5}$$

by differentiation of the ellipsoidal and quartic expressions, respectively. The incidence angle for a ray that strikes the ellipsoidal surface at (z_e, Ψ_e) can be calculated directly from the equation for the ellipse (solved for z_e in terms of Ψ_e) and its derivative (above), given an assumed value for Ψ_e. Calculation of the incidence angle at the quartic is more involved. First, we solve for the intersection of the ray with the quartic by numerically solving the quartic equation, (2.1), and the ray equation, $\Psi = \left(z-\left(-\ell_1+\ell_2\right)\right)/\cot\theta$, simultaneously to obtain (z_q, Ψ_q). The above derivative of the quartic can then be evaluated and the incidence angle calculated. The transmission coefficients for the two interfaces can then be used along with the spherical output interface transmission coefficient, T_o (see (3.3)), to obtain the total transmission coefficient for the ray. To numerically evaluate the integral in the figure-of-merit expression, (3.1), this process is repeated for values of Ψ from Ψ_0 to Ψ_1.

The figure-of-merit was calculated for a range of lens dielectric constants for *oil-lens-oil* and *oil-lens-air* designs consistent with the impedance constraints presented earlier. These data are presented in Figure III–1. All calculations assumed a coaxial input waveguide outer radius of 8.5 cm. Since both input and output impedances were matched at 100 Ω (in air), the center coaxial conductor radius was 1.6 cm (see (2.12)); and the output conductor cone angle was 21.37 degrees (see (2.15)). We observe that for both types of lens design, the figure-of-merit is a monotonically decreasing function of the lens dielectric constant. Thus, the optimum design in each case results from selection of the lowest possible dielectric constant, consistent with the constraints previously developed. We conclude that for the *oil-lens-oil* case, the dielectric constant must be greater than about 9.6, while for the *oil-lens-air* case, it must be greater than about 6.9. Since a lower dielectric constant is easier to achieve and will produce smaller reflection losses, an *oil-lens-air* design with a lens dielectric constant of about 7.0 is the optimum choice.

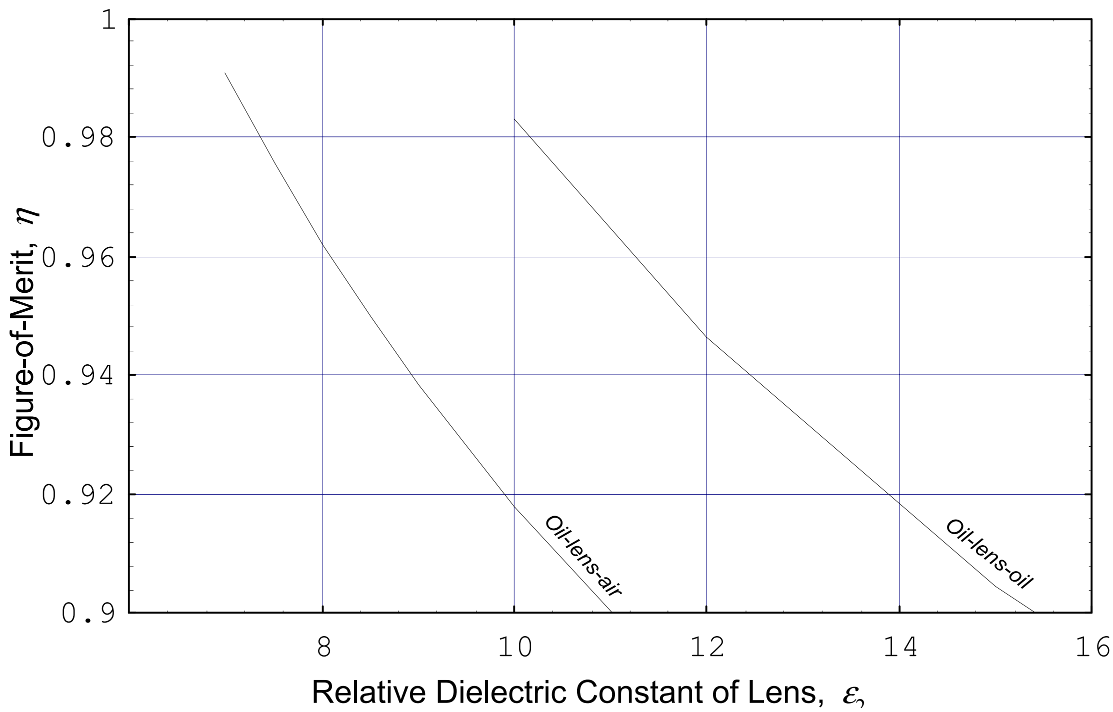

Figure III–1. Figure-of-merit for *oil-lens-oil* and *oil-lens-air* designs and an impedance of 100 Ω in air (67 Ω in oil). The dielectric constant of oil is assumed to be 2.2.

IV. Optimized Lens Designs

For both *oil-lens-oil* and *oil-lens-air* designs, we chose an output impedance of 100 Ω and an outer coaxial waveguide radius of 8.5 cm. As a result, the inner coaxial conductor radius was 1.6 cm and the flare angle of that conductor outside of the lens was 21.37 degrees. Based on the figure-of-merit calculations, we chose a lens dielectric constant of 10 for the *oil-lens-oil* design and 7 for the *oil-lens-air* design. Note that neither the impedance constraints nor the figure-of-merit calculations lead to specification of the lens output radius, Ψ_2. This remains a free parameter, subject only to the minimum introduced in [1, (3.16)], which ensures that the two lens interfaces do not intersect on axis. We used the minimum for both designs. The following table lists the parameters for both *oil-lens-oil* and *oil-lens-air* optimal lens designs. Dimensions and positions are in centimeters; angles are in degrees. The figures which follow the table (Figure IV–1 and Figure V–2) show half cross-sectional views of the two designs, including the paths for representative rays (equipotential lines) traced through the structures. The calculated figure-of-merit for the *oil-lens-oil* design is 0.981; for the *oil-lens-air* design, it is 0.991.

Lens Design Parameter	Symbol	Oil-Lens-Oil	Oil-Lens-Air
	Input Values		
Coax dielectric constant	ε_1	2.2	2.2
Lens dielectric constant	ε_2	10.0	7.0
Output dielectric constant	ε_3	2.2	1.0
Output cone angle	ϑ_0	21.37	21.37
Coax outer radius	Ψ_1	8.50	8.50
Coax inner radius	Ψ_0	1.60	1.60
Outer radius	Ψ_2	18.12	17.30
	Lens Ellipsoidal Interface		
Ellipsoid semi-major axis	a	9.63	10.27
Ellipsoid semi-minor axis	b	8.50	8.50
Ellipsoid focal distance	d	4.52	5.75
	Lens Transition Region		
Extreme ray maximum bend angle	$\theta_{1,\mathrm{max}}$	62.03	55.90
Extreme ray minimum bend angle	$\theta_{1,\mathrm{min}}$	50.26	41.41
Outer conductor flare angle	θ_1	60.96	55.45
Center conductor flare angle	θ_0	6.55	5.78
Center conductor radius at lens output	Ψ_3	1.63	1.63
	Lens Size and Proportions		
Minimum outer radius	$\Psi_{2,\mathrm{min}}$	18.12	17.30
Outer radius (input)	Ψ_2	18.12	17.30
Quartic surface to ellipsoid focal point distance	ℓ_1	14.14	16.02
	ℓ_2 / ℓ_1	0.289	0.256
	Ψ_2 / ℓ_1	1.28	1.08
	Ψ_2 / Ψ_1	2.13	2.04
	Lens On-axis Coordinates		
Ellipsoid focal point location	$-\ell_1+\ell_2$	-10.06	-11.91
Ellipsoid center	$-\ell_1+\ell_2+d$	-5.54	-6.16
Ellipsoid forward extent	$-\ell_1+\ell_2+d+a$	4.08	4.11
Quartic surface location	ℓ_2	4.08	4.11
	Some Intersections		
Ellipsoid—center conductor	(z_0, Ψ_0)	(3.91, 1.60)	(3.92, 1.60)
Coax outer conductor—lens	(z_1, Ψ_1)	(-5.34, 8.50)	(-6.06, 8.50)
Lens—quartic—ground plane	(z_2, Ψ_2)	(0.00, 18.12)	(0.00, 17.30)
Quartic—center conductor	(z_3, Ψ_3)	(4.18, 1.63)	(4.16, 1.63)
	Lens Performance		
Figure-of-Merit	η	0.981	0.991

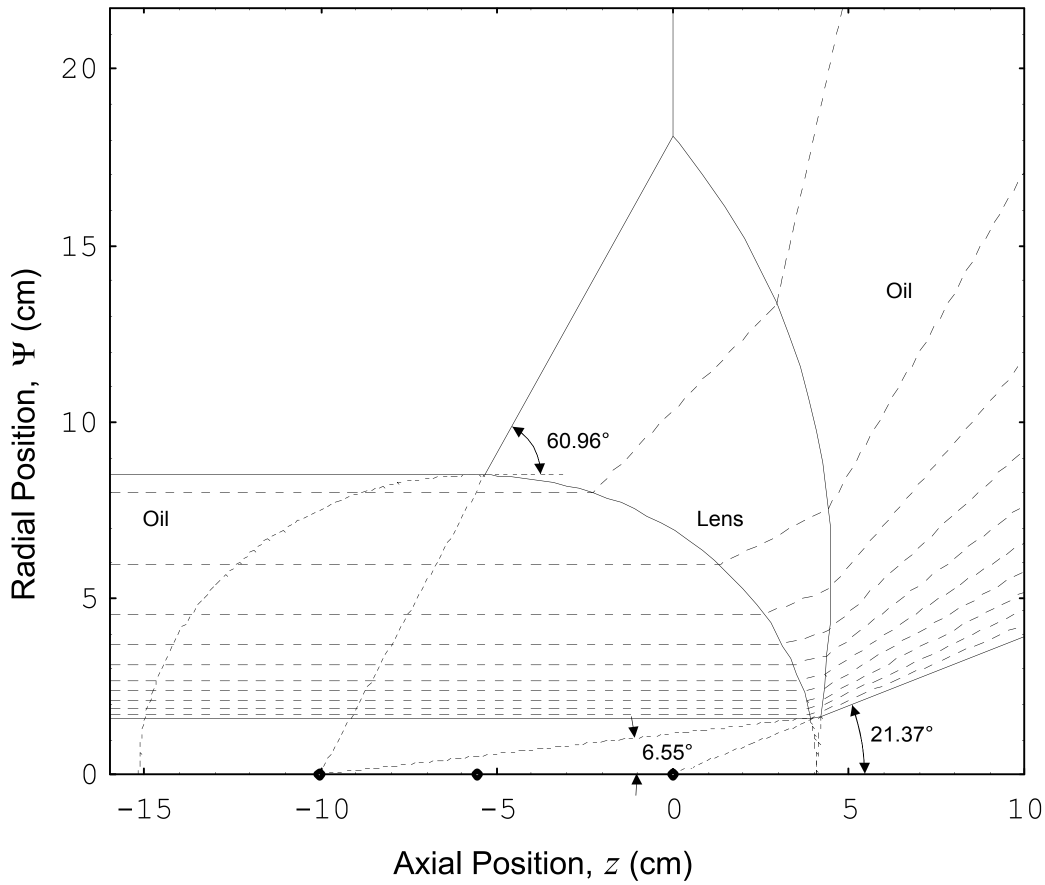

Figure IV–1. Optimized 100Ω *oil-lens-oil* design. The lens dielectric constant is 10. The figure-of-merit is 0.981.

V. Concluding Remarks

We have provided design equations and optimized designs for the feed-point lens needed to build a high-voltage half IRA. Since for both *oil-lens-oil* and *oil-lens-air* designs, the figure-of-merit decreases monotonically with increasing lens dielectric constant, the optimum choice of lens dielectric constant in an impedance matched system is one slightly larger than the minimum consistent with the condition that the required bend angle for the extreme ray at the first lens interface not exceed the maximum possible. The thickness of the lens in the axial direction scales with its output radius, which remains a free design parameter.

Since the figure-of-merit is a weak function of the dielectric constant of the lens, we are free to choose this parameter with minimal concern for its impact on lens performance. Since a lower dielectric constant is easier to achieve, and larger reflection losses accompany higher dielectric constants, the optimal design is the *oil-lens-air* design with a lens relative dielectric constant of about 7.0.

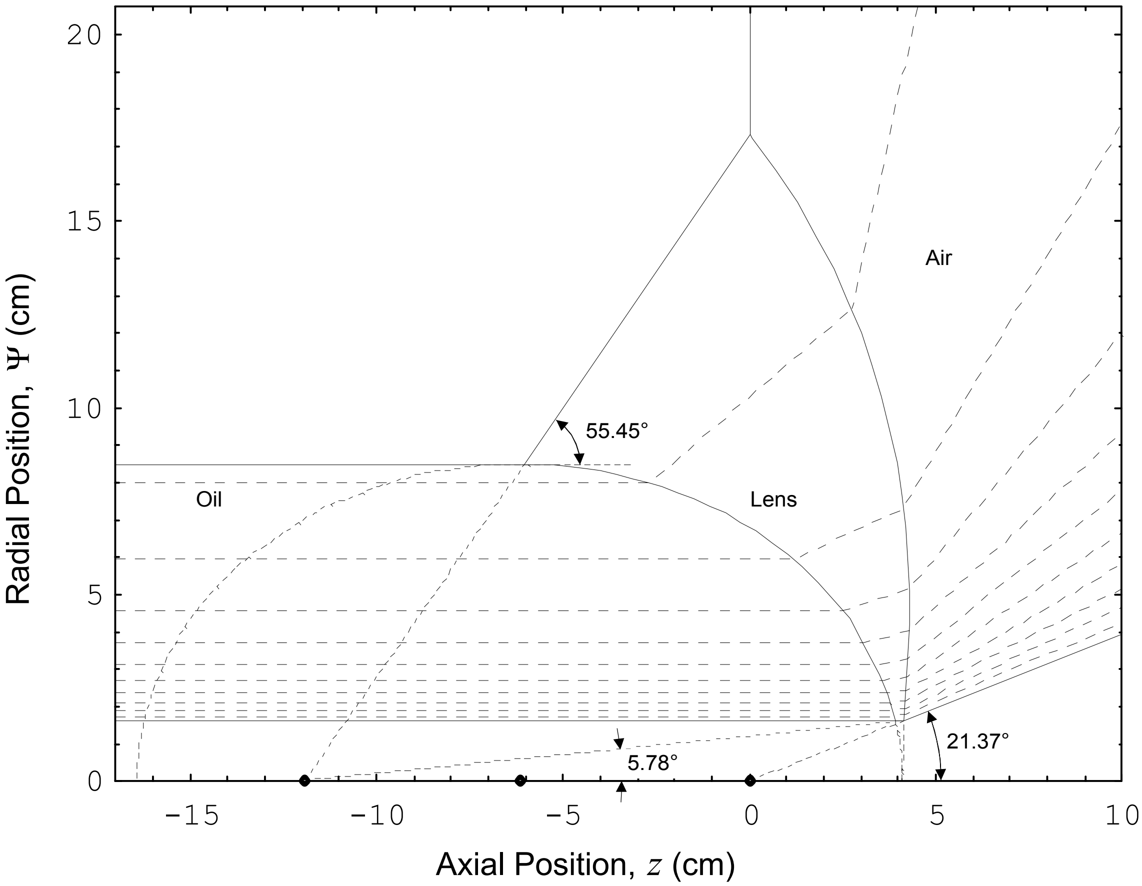

Figure V–2. Optimized 100Ω *oil-lens-air* design. The lens dielectric constant is 7. The figure-of-merit is 0.991.

Appendix A

A-I. Derivation of the Figure-of-Merit for the Half IRA Lens

We consider here a procedure for choosing the optimal design of the lens, from the family of solutions that were provided in [1]. Since the lens is symmetric about the *z*-axis, the transmission coefficient must also have the same property. Thus, all rays originating on a line of constant radius Ψ in the feed coax will penetrate the lens with the same transmission coefficient, $T_t(\Psi)$, where $T_t(\Psi)$is the total transmission coefficient through the interfaces of the lens and through the final output interface to air, if any. It is straightforward to calculate this transmission coefficient for a given lens design from the Fresnel equations.

One can now imagine an optimization procedure in which one postulates a lens configuration, calculates a figure-of-merit based on $T_t(\Psi)$, and makes adjustments to the lens to improve the figure-of-merit. We know that ideally we want T_t to be as large as possible for all Ψ, but it is unclear in what sense.

In fact, we must optimize the lens in the sense that the aperture integral of the electric field for the fast impulse is maximized. Recall that the early-time expressions for the radiated field in transmit mode and the received voltage in receive mode are

$$\begin{aligned} E_{rad}(t) &= -\frac{h_a}{2\pi r c f_g}\,\frac{dV(t)}{dt} \\ V_{rec}(t) &= -h_a\, E_{inc}(t) \end{aligned} \tag{A.1.1}$$

where f_g is the feed impedance (typically 100 Ω) divided by 377 Ω, and h_a is defined by

$$h_a = -\frac{f_g}{V_o}\iint_{S_a} E_y(x', y')\, dx'\, dy' \tag{A.1.2}$$

To optimize the radiated field and received voltage, one must maximize h_a. (One might also like a small f_g, but that is already fixed at 100 Ω/ 377Ω.)

We now have to express how h_a varies with $T_t(\Psi)$. To do so, we note that lines of constant Ψ in the feed coax must end up as lines of constant *u* in the aperture plane (Figure A:A-I–1). This must be true because in both cases we have a solution to the static Laplace's equation.

A proof that the aperture field, when there is no reflection loss, is a solution to the static Laplace's equation is in [3, Appendix A]. This solution is just the solution to the problem of a wire above a ground plane.

We therefore infer that if the fields vary with Ψ in the input coax, they must vary locally with u at the output. Thus, $T_t(\Psi) = T_t(u)$, where the relationship between Ψ and u must be determined by conformal mapping. In the section that follows, we find a conformal mapping from the coax to the aperture plane. Once that is established, we then show how to use this information to modify h_a and to derive from it a suitable figure-of-merit.

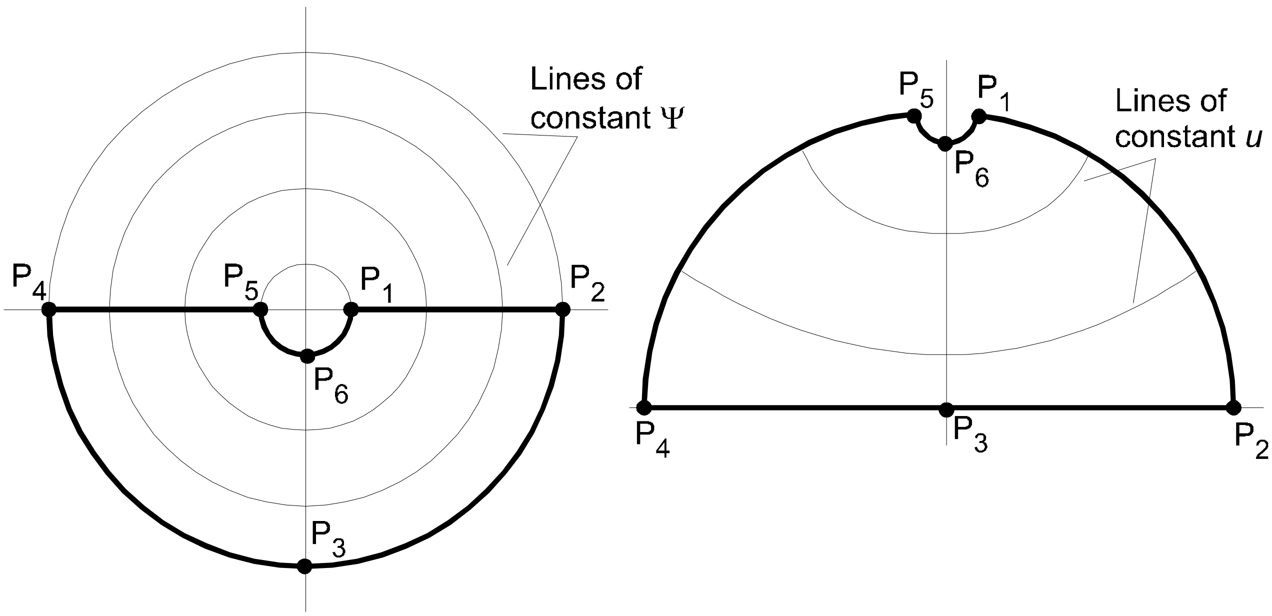

Figure A:A-I–1. The coaxial feed (left) is transformed into a geometry described by a wire above a ground plane in the aperture plane (right). Lines of constant radius in the feed coax become lines of constant u in the aperture plane.

A-II. Conformal Transformation of a Half Coax to a Wire over Ground Plane

Since the conformal transformations for a coaxial cable and for a wire above a ground plane are well understood, it is straightforward to link the two. The steps of the transformation are shown below in Figure A:A-II–1.

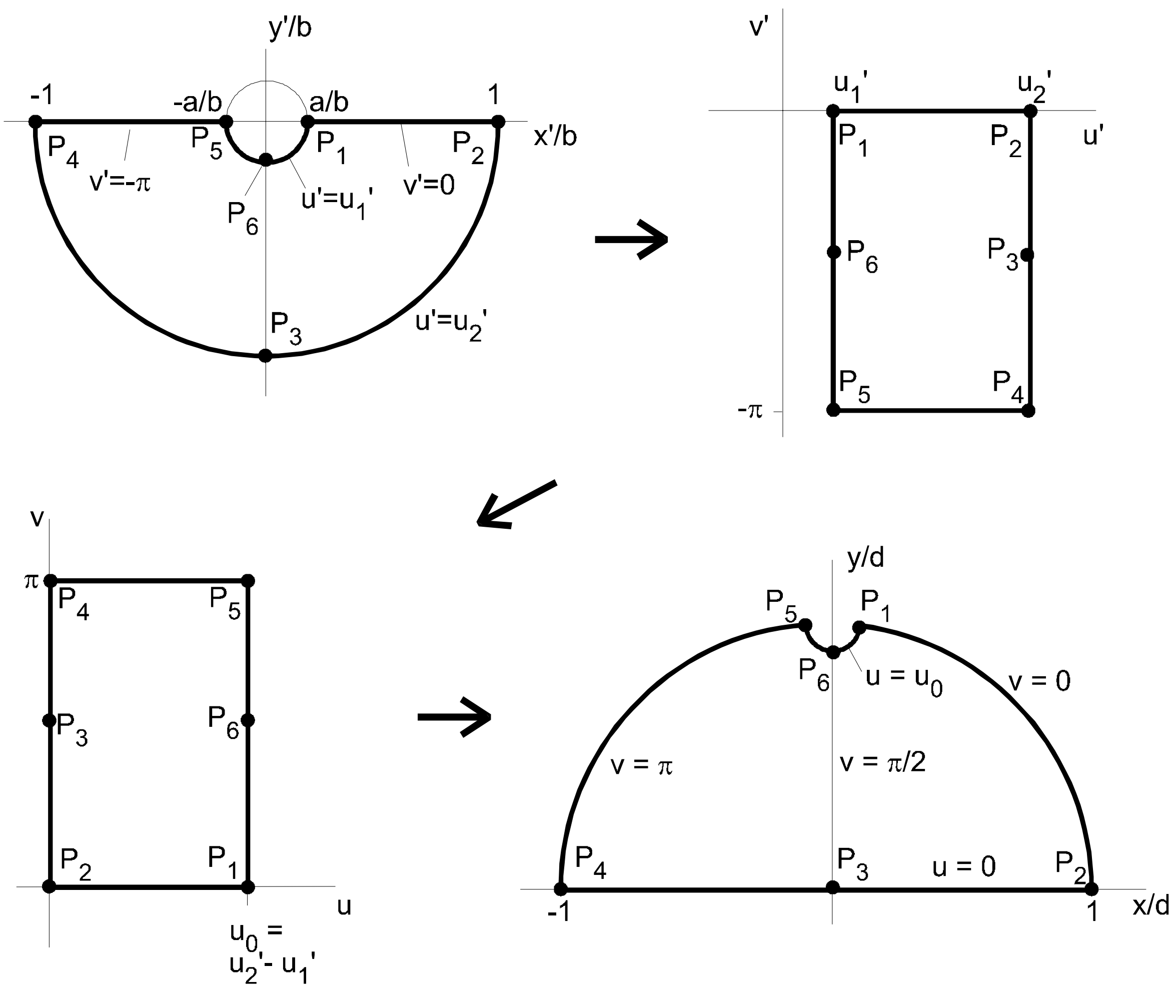

Figure A:A-II–1. The coordinate transformations required to transform a half coax to a wire above a ground plane.

We must be able to describe four coordinate systems. In the order they are used, we have

$$
\begin{aligned}
\zeta' &= x' + j\,y' \\
w' &= u' + j\,v' \\
w &= u + j\,v \\
\zeta &= x + j\,y
\end{aligned}
\qquad (A.2.1)
$$

where x, x', y, y', u, u', v and v' are all real. Note that x, y, ζ and x' y' and ζ' all have the units of meters. Furthermore, u, v, w, u', v' and w' are all dimensionless.

To find the relationship between the first and second coordinate systems, we refer to [4, p. 61], obtaining

$$
\begin{aligned}
\frac{\zeta'}{b} &= e^{w'} \\
w' &= \ln(\zeta'/b)
\end{aligned}
\tag{A.2.2}
$$

The relationship between the second and third coordinate system is just an inversion and translation. Note that the size and shape of the rectangles in the second and third coordinate systems are the same. Thus, we have

$$
w = -w' + u_2' \tag{A.2.3}
$$

Finally, the relationship between the third and fourth coordinate system can be expressed in various ways as [5]

$$
\begin{aligned}
w + j\frac{\pi}{2} &= \ln\left(\frac{\zeta/d + j}{\zeta/d - j}\right), \qquad j e^{w} = \frac{\zeta/d + j}{\zeta/d - j} \\
\frac{\zeta}{d} &= j\,\frac{e^{w + j\pi/2} + 1}{e^{w + j\pi/2} - 1} = j\,\frac{e^{w} - j}{e^{w} + j}
\end{aligned}
\tag{A.2.4}
$$

where we have shifted w by $j\pi/2$, in comparison to the usage of [5]. We have shifted w in this way in order to have $v = 0$, instead of $v = \pi/2$, on the unit circle in the aperture plane. After combining all of the above transformations, and using the relationship that $e^{u_2'} = 1$, we find a relationship between the first and last coordinate systems, i.e.,

$$
\boxed{\frac{\zeta}{d} = j\,\frac{1 - j\zeta'/b}{1 + j\zeta'/b}} \tag{A.2.5}
$$

This is the relationship we have sought.

Looking ahead, we know we will have to carry out a line integral along the line from P_6 to P_3. In the coax, this line can be expressed as

$$
\zeta' = \Psi e^{-j\pi/2} = -j\Psi \tag{A.2.6}
$$

where Ψ is the radial coordinate that varies between a and b. Substituting this into (A.2.5), we find the relationship between y in the aperture plane and Ψ in the coax along the line P_6P_3 as

$$\frac{y}{d} = \frac{1 - \Psi / b}{1 + \Psi / b} \tag{A.2.7}$$

which is valid along the line P_6P_3. The reason why we require this relationship will become apparent in the next section.

A-III. Adjustment of h_a to include Transmission Coefficient

To calculate the radiated field, we first consider the case in which the field is not perturbed by the transmission coefficient. Later, we perturb the solution by the transmission coefficient.

In the case where there is no transmission coefficient to consider, the radiated field is described by (A.1.1), with h_a calculated as in (A.1.2). It is simplest to calculate over one-half of the actual aperture, so we have

$$h_a = -\frac{2 f_g}{V_o} \iint_{S_a'} E_y(x',y')\, dx'\, dy' = -\frac{2}{\Delta v} \int_{C_a'} v(\zeta)\, dy \tag{A.3.1}$$

where S_a' is as shown in Figure A:A-III–1. Here, f_g is the input impedance for a wire above the ground plane, which is normally 100 Ω□/□377 Ω, and V_o is the voltage from the feed arm to the ground plane. The last step follows from [5 and 6].

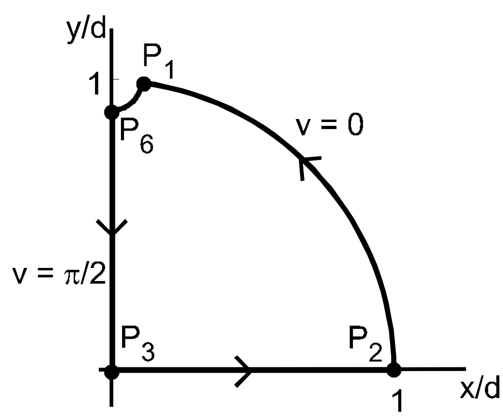

Figure A:A-III–1. The contour integral over half the aperture, C_a'.

In the absence of a perturbation due to the transmission coefficient, the contour integral is straightforward to calculate. The integral from P_3 to P_2 is zero because there is no change in *y*.

The integral from P_2 to P_1 is zero because v is zero. Finally, the integral from P_1 to P_6 is vanishingly small for thin wires. This leaves just the integral from P_6 to P_3 , which is just $-\pi d/2$. Since $\Delta v = 2\pi$, we have for the unperturbed case

$$h_a = \frac{d}{2} \tag{A.3.2}$$

This can now be used in the antenna equations, (A.1.1), to calculate the radiated field and received voltage.

Next, we consider the more interesting case of what happens when there is a perturbation in the field due to a transmission coefficient that varies as a function of position in the aperture plane. Recall that we have shown that the field in the aperture plane varies as a function of u, where lines of constant u are equipotential lines. Thus, the contour integral is modified to read

$$h_a = \frac{-2}{\Delta v} \int_{C_{63}} T_t(y)\, v(y)\, dy \tag{A.3.3}$$

where C_{63} is the straight-line contour from P_6 to P_3. This expression assumes that the field is affected only locally by the transmission coefficient, an assumption which is valid at high frequencies. As before, $v(y) = \pi/2$ on the contour, and $\Delta v = 2\pi$; so we have the simplified result

$$h_a = -\frac{1}{2} \int_{C_{63}} T_t(y)\, dy \tag{A.3.4}$$

Note that $T_t(y)$ includes transmission coefficients for <u>*all*</u> interfaces, including the final oil-air interface implied by an *oil-lens-oil* design. That final interface introduces no additional y-dependence, however, as we assume it is spherical and concentric with the emerging wavefront. To simplify the above expression even further, we note that we can express $T_t(y)$ in terms of Ψ in the coax feed. Thus, we have

$$\begin{aligned} \frac{y}{d} &= \frac{1-\Psi/b}{1+\Psi/b}\,, \qquad \frac{dy}{d} = \frac{-2}{(1+\Psi/b)^2}\,\frac{d\Psi}{b} \\ \frac{dy}{d\Psi} &= -2\frac{d}{b}\,\frac{1}{(1+\Psi/b)^2} \\ h_a &= -\frac{1}{2}\int_{C_{63}} T_t(\Psi)\,\frac{dy}{d\Psi}\,d\Psi \end{aligned} \tag{A.3.5}$$

where we have used (A.2.7) to relate y to Ψ. Note that C_{63} is now the contour in the coax from P_6 to P_3, as shown in the first sketch of Figure A:A-II–1. This is simplified to

$$h_a = \frac{d}{b} \int_a^b \frac{T_t(\Psi)}{(1 + \Psi / b)^2} \, d\Psi \tag{A.3.6}$$

This is the final result we have sought. Note in this expression that $h_a = h_{a,oil}$ is normalized to a plane of reference in oil. If we used a plane of reference in air, we would recover the unperturbed result of (A.3.2), $h_{a,air} = d/2$.

A suitable figure-of-merit for our candidate lens configurations may now be defined as

$$\eta = \frac{h_{a,oil}}{h_{a,oil}^{(opt)}} \tag{A.3.7}$$

where $h_{a,oil}^{(opt)}$ is the value of the aperture integral, normalized to a plane of reference in oil, that would be observed if there were no power losses in the transition from oil in the coax to air. We derive below this optimal aperture integral.

Recall from (A.3.1) that h_a is inversely proportional to the voltage. If we assume that the an optimal transition between oil and air would be a smooth transition region with no power loss, then the power in oil and in air would be the same and we could write

$$\frac{h_{a,oil}^{(opt)}}{h_{a,air}} = \frac{V_{air}}{V_{oil}^{(opt)}} = \sqrt{\frac{Z_{c,air}}{Z_{c,oil}}} \tag{A.3.8}$$

since the voltage is proportional to the square root of the power–impedance product. Now, since the impedance is proportional to the square root of the dielectric constant, and the relative dielectric constant of air is 1.0, we have

$$h_{a,oil}^{(opt)} = (d/2) \sqrt[4]{\varepsilon_{oil}} \tag{A.3.9}$$

where we have used $h_{a,air} = d/2$, and ε_{oil} is the relative dielectric constant of oil.

Combining the expressions obtained above, we finally obtain as our lens figure-of-merit

$$\boxed{\eta = \frac{2/b}{\sqrt[4]{\varepsilon_{oil}}}\int_a^b \frac{T_t(\Psi)}{(1+\Psi/b)^2}\,d\Psi} \tag{A.3.10}$$

Recall that for each candidate lens configuration we can calculate a total transmission coefficient as a function of Ψ in the oil-filled feed coax. It has until now been unclear how to weigh the contributions of each ray to the overall radiated field. The above expression tells us how to weigh that contribution. It is therefore the figure-of-merit for the candidate lens configuration.

Acknowledgments

We would like to thank Mr. William D. Prather of Phillips Laboratory for funding this work. We would also like to thank Dr. Carl E. Baum for his many helpful discussions which contributed to this work.

References

1. E. G. Farr and C. E. Baum, Feed-Point Lenses for Half Reflector IRAs, Sensor and Simulation Note 385, November 1995.

2. C. A. Balanis, *Advanced Engineering Electromagnetics*, New York, John Wiley & Sons, 1989, p. 191.

3. E. G. Farr and C. E. Baum, A Simple Model of Small-Angle TEM Horns, Sensor and Simulation Note 340, May 1992.

4. P. Moon and D. E. Spencer, *Field Theory Handbook*, Second Edition, Corrected Third Printing, Springer-Verlag, New York, 1988, p. 61.

5. E. G. Farr, Optimizing the Feed Impedance of Impulse Radiating Antennas, Part I, Reflector IRAs, Sensor and Simulation Note 354, January 1993.

6. C. E. Baum, Aperture Efficiencies for IRAs, Sensor and Simulation Note 328, June 1991.